VOLUME 10 ISSUE 2 2024

ISSN 2454 – 3055

INTERNATIONAL JOURNAL OF ZOOLOGICAL INVESTIGATIONS

Forum for Biological and Environmental Sciences

Published by Saran Publications, India

International Journal of Zoological Investigations Vol. 10, No. 2, 1484-1502 (2024)

International Journal of Zoological Investigations
Contents available at Journals Home Page: www.ijzi.net
Editor-in-Chief: Prof. Ajai Kumar Srivastav
Published by: Saran Publications, Gorakhpur, India

ISSN: 2454-3055

Melatonin a Multi-Target Inhibitor: Unveiled its Anticancer Potential through DFT and Molecular Docking Studies with Key Oncogenic Proteins

Sharma Anupam[1], Katual Manoj Kumar[2], Tiwari Neha[2], Bose J.C.[3], Upadhyay Sushil Kumar[4]* and Sharma Anil Kumar[5]

[1]Department of Physics, Guru Kashi University, Talwandi Sabo, Bathinda 151302, Punjab, India
[2]Department of Pharmaceutical Sciences, Guru Kashi University, Talwandi Sabo, Bathinda 151302, Punjab, India
[3]Department of Biotechnology, Chandigarh University Gharuan, Mohali, Punjab, India
[4]Department of Bio-Sciences and Technology, MMEC, Maharishi Markandeshwar (Deemed to be University), Mullana-Ambala 133207, Haryana, India
[5]Department of Biotechnology, Amity School of Biological Sciences, Amity University Punjab, Mohali140306, Punjab, India

**Corresponding Author*

Received: 12th November, 2024; **Accepted:** 22nd December, 2024; **Published online:** 30th December, 2024

https://doi.org/10.33745/ijzi.2024.v10i02.150

Abstract: The hormone melatonin, which is well-known for controlling circadian cycles, has recently drawn interest due to possible anticancer effects. In order to examine the electronic structure, optimized geometry, and molecular characteristics of melatonin that contribute to its biological action, we give a thorough Density Functional Theory (DFT) analysis of the hormone at the B3LYP level of theory using the 6-311G (d,p) basis set. The calculated molecular descriptors, including the bond angles and lengths, vibrational frequencies and IR spectra, electrostatic potential, and HOMO-LUMO energy gap, Mulliken atomic charges provide information about the stability and chemical reactivity of melatonin in biological systems. Keeping in view its stability and suitability for biological and pharmaceutical applications, we have performed molecular docking to check its binding affinity to important cancer-related protein targets, such as MMP13 collagenase-3, matrix metalloproteinase-9 (MMP-9), epidermal growth factor receptor (EGFR), and NUDT5_HUMAN (ADP-sugar pyrophosphatase). With binding scores ranging from -8.2 to -7.3 kcal/mol, the docking results showed significant binding interactions, indicating that melatonin (MTN) has a considerable potential to inhibit key proteins which are responsible in the development and spread of cancer. Notably, MMP-9 and MMP13 collagenase-3, two proteins strongly linked to tumour growth and cancer cell invasion, showed favourable binding affinities to melatonin.

Keywords: Melatonin, MMP13 collagenase-3, Matrix metalloproteinase-9 (MMP-9), Epidermal growth factor receptor (EGFR), NUDT5_HUMAN (ADP-sugar pyrophosphatase)

Citation: Sharma Anupam, Katual Manoj Kumar, Tiwari Neha, Bose J.C., Upadhyay Sushil Kumar and Sharma Anil Kumar: Melatonin a multi-target inhibitor: Unveiled its anticancer potential through DFT and molecular docking studies with key oncogenic proteins. Intern. J. Zool. Invest. 10(2): 1484-1502, 2024.

https://doi.org/10.33745/ijzi.2024.v10i02.150

Introduction

The neurohormone melatonin, which is mostly produced by the pineal gland, has gained notice for its function in controlling sleep-wake cycles and circadian rhythms. Aaron Lerner removed melatonin which is also known as 5-methoxy-N-acetyltryptamine, from cow pineal in 1958. Since Aaron Lerner and others discovered it in the 1950s (Lerner *et al*., 1958), a lot of study has been done to clarify its diverse physiological and pharmacological effects. In addition to being essential for controlling sleep, melatonin also affects mood, the immune system, and even the ageing process (Reiter *et al*., 2016). Early research showing melatonin's effects on sleep induction and phase shifting of the sleep-wake cycle (Arendt, 1998) established the hormone's basic function in circadian rhythm regulation. More recent studies have looked into the therapeutic uses of melatonin outside of sleep disorders, such as the treatment of jet lag, seasonal affective disorder (SAD), and insomnia (Checkley *et al*., 1993; Herxheimer and Petrie, 2002). Furthermore, some investigations have demonstrated the antioxidant qualities of melatonin and its capability to alleviate disorders associated with oxidative stress (Hardeland *et al*., 2011).

Meatonin (MTN) has potent antioxidant qualities that guard against oxidative damage. Several studies have looked into how melatonin affects diseases and injuries to the liver. Melatonin may control a number of cellular pathways in diverse pathophysiological scenarios, including autophagy, proliferation, apoptosis, inflammation, and metastasis. Melatonin may be utilized to treat and prevent conditions and damage of the liver (Zhang *et al*., 2017). MTN's antioxidant qualities save bodily tissues and cells from oxidative damage. Because of its anti-inflammatory, anti-oxidant, anti-infective, anti-tumor characteristics. MTN controls blood flow in humans. Melatonin is essential for the resynchronization of biological cycles, the onset and maintenance of sleep, and for the treatment of rheumatologic, metabolic, and retinal disorders. Melatonin is also having anti-inflammatory, anti-oxidative, and immuno-modulatory effects. Melatonin is not recognized as a viricidal drug; however, it has been proposed to reduce viral infections because of these qualities as well as its non-toxic nature (Vlachou *et al*., 2021)

Empirical research indicates that melatonin plays a significant role in both preventing and treating breast cancer (Coleman and Reiter, 1992). Patients with breast cancer had a more than 50% reduction in the circadian amplitude of melatonin compared to patients with nonmalignant breast illness (Touitou *et al*., 1993). Urine samples taken in the morning have shown elevated levels of melatonin in patients with breast cancer (Bartsch *et al*., 1981). Furthermore, melatonin has been investigated as a potential treatment for a number of different ailments, such as cancer, migraines, and seasonal affective disorder (Claustrat *et al*., 2005). Melatonin's antioxidant qualities are especially notable since it can up regulate antioxidant enzymes and scavenge free radicals, sparing cells from oxidative damage (Tan *et al*., 2007). Moreover, the identification of melatonin receptors in several peripheral organs implies that the impact of melatonin surpasses the regulation of sleep, as it may have implications for immuno-logical response, metabolism, and cardiovascular health (Dubocovich *et al*., 2010). Despite these developments, research on the entire range of melatonin's effects and mechanisms of action is still ongoing. Melatonin, for example, has a well-established function in regulating sleep, although its impact on mood disorders and cognitive performance has still to be studied (Srinivasan *et al*., 2006).

Various diseases, such as diseases related to cardiovascular system, COVID-19 and cancers are found to be linked with insufficient release of MTN (Imenshahidi *et al*., 2020; Nishi *et al*., 2020; Rebollo-Hernanz *et al*., 2020). If there is a gap between the body's ability to remove reactive oxygen species (ROS) and the production of them, then it will result in oxidative stress (Talib *et al*., 2021). As one of nature's most potent anti-

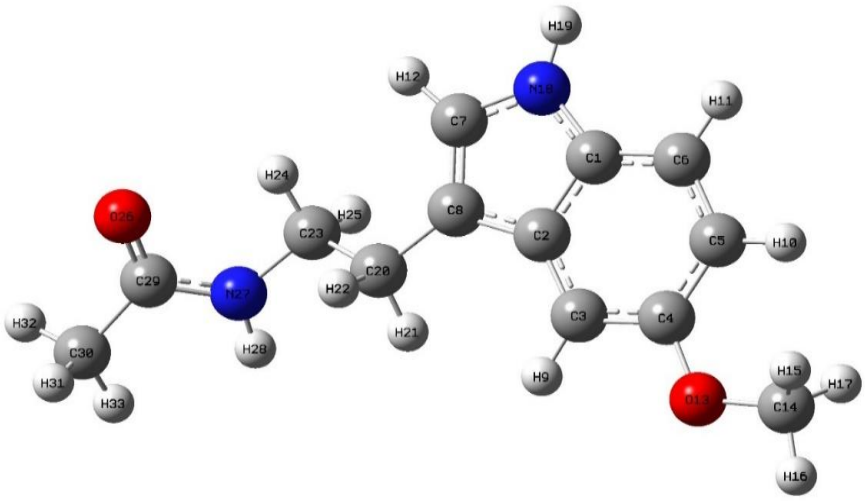

Fig. 1: Optimised structure of melatonin computed with DFT(B3LYP) at 6-311G(d,p) level.

oxidants, it affects both the cellular antioxidant enzyme system and reactive oxygen and nitrogen species (Cecon *et al*., 2018). It binds up to 10 free radicals per molecule, contrary to some conventional antioxidants (Bonomini *et al*., 2018). Because of its anti-inflammatory, anti-oxidant, anti-infective, and anti-tumor qualities, MTN has been the subject of much research on its therapeutic and protective role in controlling human haemostasis (Vlachou *et al*., 2021).

The complex hormone melatonin has important effects on human health. The necessity for more investigation into its mechanisms of action and wider health advantages is highlighted by the ongoing study into its therapeutic potential across a variety of fields. The prospect of using melatonin for a variety of medical procedures is becoming more and more likely as our knowledge of its uses and functions expands. Our purpose in this paper was to find out the chemical properties of melatonin with the help of chemical computations and to check its properties as cancer inhibitor.

Materials and Methods

The molecular structures were drawn by using G-03W and GAUSS VIEW 6.0.16 VERSION (6) of ab-initio quantum mechanical program (Frich *et al*., 2005; Sharma *et al*., 2019). The density functional theory (DFT) was used at B3LYP level with 6-311G(d,p) basis set in the neutral gas phase geometry to optimize the compound. Figure 1 shows the optimized structures of melatonin when 6-311G(d,p) basis set is used at B3 LYP level. This structure consists of 33 atoms and has 93 modes of vibrations. The molecular structure of the compound consist of 34 bond lengths, 58 bond angles and 76 dihedral angles. DFT was used in this study at B3LYP level with 6-311G(d,p) basis set to investigate the electronic properties of melatonin. The optimized structure was used to calculate the Bond lengths, Mullikan atomic charges, electrostatic potential surfaces, vibrational frequencies (scaled 0.9614), IR spectra and HOMO-LUMO energy gaps. For completing docking assignments we have used mcule.com (https://mcule.com). Melatonin structure for docking is taken from drug bank (https://go.drugbank.com). BIOVIA Discovery studio is used for visualisation purpose (https://www.3ds.com).

Results and Discussion

Bond Lengths

DFT was used at B3LYP level along with 6-311G (d, p) basis set to study Bond lengths of Melatonin.

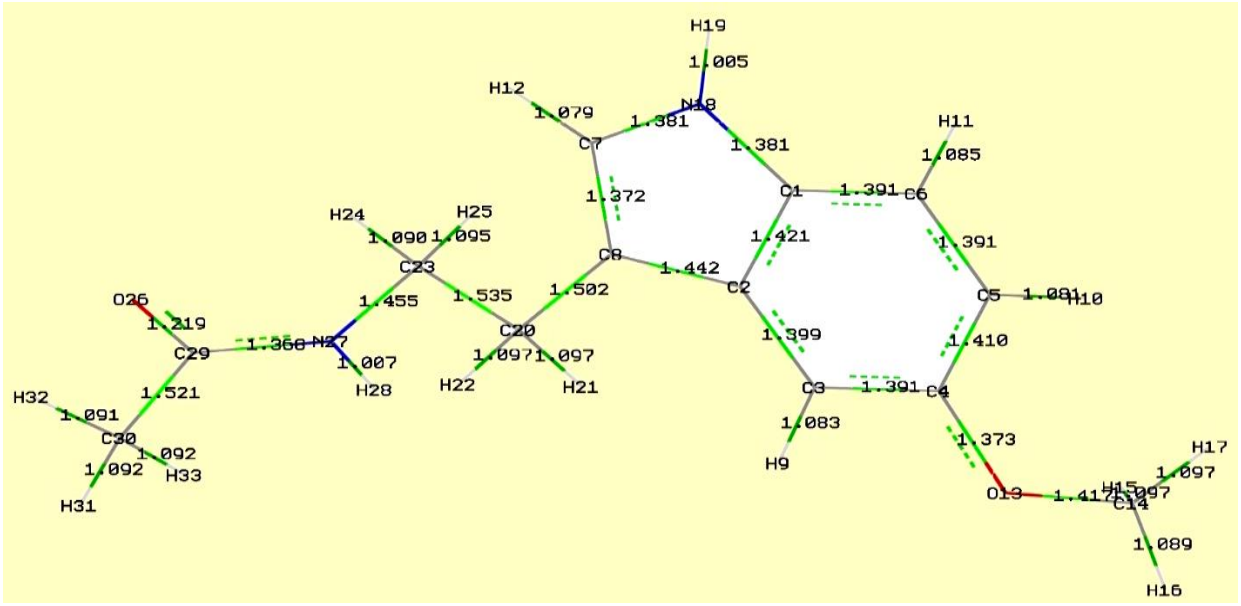

Fig. 2: Bond length (A^0) values of melatonin computed with DFT(B3LYP) at 6-311G(d,p) level.

The calculated values of the bond lengths are in the units of 'A^0' which have been shown in Figure 2. When we investigated the bond lengths, it was noted that the bond length order is C20-C23 (1.5349 A^0) >C29-C30 (1.5209 A^0) >C8-C20 (1.5023 A^0)> C23-N27 (1.4554 A^0)>C2-C8 (1.4423)> C1-C2 (1.4208 A^0)> O13-C14 (1.4166 A^0) > C4-C5 (1.4102 A^0). These values showed that the highest reactive sites will be around these bonds. Hence, there is a possibility of nucleophilic or electrophilic attack on these positions. The bond length values between C1-C2, C2-C3, C3-C4, C4-C5, C5-C6, C1-C6 are found 1.4208 Å, 1.3994 Å , 1.3912 Å , 1.4102 Å, 1.3915 Å and 1.3913 Å, respectively. Actual bond length values of C-C and C=C in benzene ring is same that is 1.39 Å because of its aeromaticity. The distortion in the structure is due to the steric effect of the functional groups in melatonin which include CH_3O group on the phenyl ring, CH_3CONH group and the indole group.

Geometric parameters, bond angles and dihedral angles are calculated by B3LYP/6-311G (d, p). Earlier studies suggest that Amide bonds are the most common structural element in organic molecules and biomolecules. Amide bonds are special because they can form resonant structures, which make them extremely stable and allow them to adopt specific three-dimensional forms that ultimately decide their roles (Mahesh *et al*., 2018). The amide bond is one of the most common chemical bonds which may be found in a large number of compounds and biomolecules (Greenberg *et al.,* 2000; Hughes, 2009; Brunton *et al.,* 2010; Pattabiraman and Bode, 2011; Brown and Bostrom, 2016). Because amide bonds are highly stable under a variety of reaction circumstances, including basic and acidic ones, high temperatures, and the presence of other compounds, nature has employed them to create these significant biomolecules (Kaspar and Reichert, 2013). A resonant structure that gives the amide CO-N bond a double bond character is thought to be responsible for the great stability of amide bonds (Thorner *et al*., 2000). In case of melatonin Amide linkage bond angle A50 (O26, C29, N27) has been found to be 123.0661 when calculated with DFT (B3LYP) at 6-311G (d, p) level. The amide bonds' planar structure increases resonance, which enhances its stability and reduces reactivity, especially when interacting with biological targets. Due to sp^2 hybridization, angles within the indole ring are around 120° as shown in Table 1 and it has a planar structure. Due to this planar structure it has aromatic stability

Table 1: Bond angles of melatonin computed with DFT (B3LYP) at 6-311G (d, p) level

Symbols	Bond angles (⁰)	Symbols	Bond angles (⁰)	Symbols	Bond angles (⁰)
A1 (C2,C1,C6)	121.597	A20 (C8,C7,N18)	110.203	A39 (H21,C20,C23)	108.9563
A2 (C2,C1,N18)	107.146	A21 (H12,C7,N18)	120.0492	A40 (H22,C20,C23)	108.3582
A3 (C6,C1,N18)	131.258	A22 (C2,C8,C7)	106.2396	A41 (C20,C23,H24)	110.6081
A4 (C1,C2,C3)	119.284	A23 (C2,C8,C20)	125.84	A42 (C20,C23,H25)	109.8897
A5 (C1,C2,C8)	107.344	A24 (C7,C8,C20)	127.9104	A43 (C20,C23,N27)	112.7648
A6 (C3,C2,C8)	133.372	A25 (C4,O13,C14)	118.6689	A44 (H24,C23,H25)	108.0777
A7 (C2,C3,C4)	119.196	A26 (O13,C14,H15)	111.8141	A45 (H24,C23,N27)	105.8135
A8 (C2,C3,H9)	122.110	A27 (O13,C14,H16)	105.8749	A46 (H25,C23,N27)	109.5172
A9 (C4,C3,H9)	118.694	A28 (O13,C14,H17)	111.8253	A47 (C23,N27,H28)	118.4007
A10 (C3,C4,C5)	120.827	A29 (H15,C14,H16)	109.0468	A48 (C23,N27,C29)	122.8696
A11 (C3,C4,O13)	115.523	A30 (H15,C14,H17)	109.1406	A49 (H28,N27,C29)	118.6633
A12 (C5,C4,O13)	123.650	A31(H16,C14,H17)	109.0333	A50 (O26,C29,N27)	123.0661
A13 (C4,C5,C6)	120.744	A32 (C1,N18,C7)	109.0675	A51 (O26,C29,C30)	121.6564
A14 (C4,C5,H10)	120.428	A33 (C1,N18,H19)	125.7415	A52 (N27,C29,C30)	115.2774
A15 (C6,C5,H10)	118.827	A34 (C7,N18,H19)	125.1849	A53 (C29,C30,H31)	108.5513
A16 (C1,C6,C5)	118.352	A35 (C8,C20,H21)	108.9274	A54 (C29,C30,H32)	108.5188
A17 (C1,C6,H11)	121.515	A36 (C8,C20,H22)	110.5167	A55 (C29,C30,H33)	113.9919
A18 (C5,C6,H11)	120.133	A37 (C8,C20,C23)	113.8169	A56 (H31,C30,H32)	107.4225
A19 (C8,C7,H12)	129.747	A38 (H21,C20,H22)	105.9605	A57 (H31,C30,H33)	108.9575
				A58 (H32,C30,H33)	109.1983

which makes it less prone to reactivity under physiological conditions.

Methoxy group bond angles which are more deviated from planar structure are A26 (O13, C14, H15), A27 (O13, C14, H16) , A28 (O13,C14,H17), A29 (H15,C14,H16), A30 (H15,C14,H17), and A31(H16,C14,H17), which indicates areas of torsional strain. So attached methoxy group is one of the potential reactive sites in melatonin. Deviation from planar structure can also be seen in amine bond i.e. A2 (C2,C1,N18), A3 (C6,C1,N18), A32 (C1,N18,C7), A33 (C1,N18,H19) and A34 (C7,N18,H19) which shows that it is also one of site of torsional strain. Torsional strain can be seen in the angles with C23 as acetamide group CH_3CONH is attached with C23. Due to this reason the angle A37 (C8,C20,C23), A39 (H21,C20,C23), A40 (H22,C20,C23), A41 (C20,C23,H24), A42 (C20,C23,H25), A43 (C20,C23,N27), A44 (H24,C23,H25), A45 (H24,C23,N27) and A46 (H25,C23,N27) show deviation from planar structure. This deviation from planar structure is responsible for reactivity of melatonin.

Dihedral Angles

The torsional strain in the molecule can affect both stability and reactivity, is revealed by dihedral angles. The C-C bond that joins the indole ring to the acetamide group and the C-N bond in the amide linkage are two important dihedral angles in melatonin. The dihedral angle around the C-N bond is often close to 0° or 180°, indicating a planar conformation. This planar structure is stabilized by resonance, making the amide group less reactive. However, any deviation from planarity can increase torsional strain and potential reactivity, especially under enzymatic

conditions. The relative configuration of the acetamide group and the indole ring is determined by the dihedral angle surrounding this bond. To maximize conjugation between the two groups, a coplanar conformation would have a dihedral angle of about 0° or 180°. However, steric interactions caused by a non-zero dihedral angle have a tendency to destabilize the molecule and enhance its reactivity, especially when electrophilic species are involved. As it is clear from the Table 2 that some of the dihedral are not around 0° or 180 which shows that the melatonin molecule has torsional strain sites with increased potential reactivity.

Vibrational Assignments

To study melatonin's interactions, stability, and reactivity, it is required to understand its structural and dynamic properties, which can only be obtained through vibrational analysis. Vibrational frequencies obtained by using DFT, usually tell full information on the molecule's normal modes. Through these computations, we are able to interpret experimental Raman and infrared (IR) spectra, identify functional groups, and evaluate the impact of different substituents on melatonin's vibrational properties. Vibrational Frequencies/PED calculated at DFT6-311G (d, p)/B3LYP level are shown in Table 3. Because melatonin contains several functional groups, such as the amide bond, methoxy group, indole ring, and aliphatic chains, it has a complex vibrational spectrum.

There were actually 3N-6 typical modes of vibration for a non-linear molecule with N atoms (Kemnitz and Loewen, 2007), displayed the 33 atoms and 93 vibrational modes of melatonin, which include 34 stretching, 31 bending, 27 torsion, and 1 out-of-plane vibration. For the neutral state, each vibrational mode's TED assignment was calculated. The computed frequencies of melatonin were fitted using a scaling factor of 0.9613 for DFT (RB3LYP)/6-311G (d, p) and corresponding IR spectrum is shown in Figure 3. The fingerprint region is located on the left side, below 1000 cm^{-1} to 400 cm^{-1}, while the functional group region is located on the right side, above 1000 to 4000 cm^{-1}. The right portion has comparatively few peaks above 2000 cm^{-1}. This area of the spectrum did, however, include some diagnostic data. In this area, a fairly wide peak between 3100 cm^{-1} and 3600 cm^{-1} indicates the total number of protons that can be exchanged, usually from carboxylic acid, alcohol, amine, or amide groups (Mujika *et al*., 2005).

Three components make up the structure of melatonin: (a) the methoxy group OCH_3, (b) the acetyl ethylamine side chain, and (c) the heterocyclic system of indole. The vibrations in melatonin are basically due to these three groups. N–H stretching vibrations are typically found between 3500 and 3300 cm^{-1} (Wang and Cao, 2011). The amide NH stretching show up at 3495 cm^{-1} and the indole NH stretching vibration appeared between 3522 cm^{-1} and 3526 cm^{-1} in the gas phase experimental IR spectra (Bisong *et al*., 2020). The vibrational strectching frequency of indole NH (18N-19H) and amide NH (27N-28H) was found 3680.94 cm^{-1}, and 3634.77 cm^{-1}, respectively which are very close to the experimental values. The Intensity of (indole) 18N-19H stretching is more as compared to (amide) 27N-28H stretching. The PED% in the stretching mode of vibration is 100% (Table 3).

The C-H stretching of aromatic, alkyl, and methyl were found in the range from 2991.26 cm^{-1} to 3245.3 cm^{-1}. The C-C vibrational stretching in a ring usually occurs in a 1400-1600 cm^{-1} region (Altun *et al*., 2003; Tarı and Aydemir, 2023). It was noted that C-C stretching vibrational frequencies for 1C-6C, 2C-3C, 6C-5C and 1C-6C were 1673.2 cm^{-1}, 1619.77 cm^{-1}, 1489.47 cm^{-1} and 1379.48 cm^{-1}, respectively. The significant vibration in both rings of melatonin has been found in the range of 1300–1700 cm^{-1}. The range of vibrational frequencies of the carbon-carbon single bond is 1379.48 cm^{-1}-1673.2 cm^{-1}. C=C stretching vibrations are observed around 1591.21 cm^{-1}, which indicates the aromatic stability and contributes to the overall rigidity of the indole in melatonin. These frequencies match earlier

Table 2: Electronic structure parameter, dihedral angles of melatonin calculated with DFT(B3LYP) at 6-311G(d,p) level

Symbols	Dihedral angles (^{0})	Symbols	Dihedral angles (^{0})
D1(C6,C1,C2,C3)	0.1784	D39(C8,C7,N18,C1)	0.0899
D2(C6,C1,C2,C8)	-179.8031	D40(C8,C7,N18,H19)	179.2344
D3(N18,C1,C2,C3)	-179.9036	D41(H12,C7,N18,C1)	179.7849
D4(N18,C1,C2,C8)	0.1149	D42(H12,C7,N18,H19)	-1.0706
D5(C2,C1,C6,C5)	-0.0659	D43(C2,C8,C20,H21)	-37.9788
D6(C2,C1,C6,H11)	179.9817	D44(C2,C8,C20,H22)	78.0424
D7(N18,C1,C6,C5)	-179.9616	D45(C2,C8,C20,C23)	-159.7646
D8(N18,C1,C6,H11)	0.0859	D46(C7,C8,C20,H21)	143.3322
D9(C2,C1,N18,C7)	-0.126	D47(C7,C8,C20,H22)	-100.6467
D10(C2,C1,N18,H19)	-179.2646	D48(C7,C8,C20,C23)	21.5464
D11(C6,C1,N18,C7)	179.7811	D49(C4,O13,C14,H15)	61.1284
D12(C6,C1,N18,H19)	0.6425	D50(C4,O13,C14,H16)	179.7664
D13(C1,C2,C3,C4)	-0.2072	D51(C4,O13,C14,H17)	-61.6059
D14(C1,C2,C3,H9)	179.6042	D52(C8,C20,C23,H24)	-62.6445
D15(C8,C2,C3,C4)	179.7685	D53(C8,C20,C23,H25)	56.604
D16(C8,C2,C3,H9)	-0.4201	D54(C8,C20,C23,N27)	179.0917
D17(C1,C2,C8,C7)	-0.0614	D55(H21,C20,C23,H24)	175.5857
D18(C1,C2,C8,C20)	-178.9841	D56(H21,C20,C23,H25)	-65.1658
D19(C3,C2,C8,C7)	179.9608	D57(H21,C20,C23,N27)	57.3219
D20(C3,C2,C8,C20)	1.0381	D58(H22,C20,C23,H24)	60.7313
D21(C2,C3,C4,C5)	0.1315	D59(H22,C20,C23,H25)	179.9798
D22(C2,C3,C4,O13)	-179.8991	D60(H22,C20,C23,N27)	-57.5325
D23(H9,C3,C4,C5)	-179.6864	D61(C20,C23,N27,H28)	-67.1804
D24(H9,C3,C4,O13)	0.283	D62(C20,C23,N27,C29)	109.8117
D25(C3,C4,C5,C6)	-0.0191	D63(H24,C23,N27,H28)	171.7836
D26(C3,C4,C5,H10)	179.9393	D64(H24,C23,N27,C29)	-11.2242
D27(O13,C4,C5,C6)	-179.986	D65(H25,C23,N27,H28)	55.5159
D28(O13,C4,C5,H10)	-0.0276	D66(H25,C23,N27,C29)	-127.4919
D29(C3,C4,O13,C14)	-179.5249	D67(C23,N27,C29,O26)	1.8497
D30(C5,C4,O13,C14)	0.4436	D68(C23,N27,C29,C30)	-178.0882
D31(C4,C5,C6,C1)	-0.0143	D69(H28,N27,C29,O26)	178.8343
D32(C4,C5,C6,H11)	179.9389	D70(H28,N27,C29,C30)	-1.1036
D33(H10,C5,C6,C1)	-179.9733	D71(O26,C29,C30,H31)	-63.3114
D34(H10,C5,C6,H11)	-0.0202	D72(O26,C29,C30,H32)	53.1428
D35(H12,C7,C8,C2)	-179.6724	D73(O26,C29,C30,H33)	175.0583
D36(H12,C7,C8,C20)	-0.7793	D74(N27,C29,C30,H31)	116.6275
D37(N18,C7,C8,C2)	-0.0157	D75(N27,C29,C30,H32)	-126.9183
D38(N18,C7,C8,C20)	178.8774	D76(N27,C29,C30,H33)	-5.0028

Table 3: Frequencies/PED%s calculated at DFT6-311G (d, p)/B3LYP level

S. No.	Intensity km/mol	Frequency (cm^{-1})	Assignments	Atom No.	PED%
s1	75.29	3680.94	STRE	18N-19H	s1 100
s2	17.06	3634.77	STRE	27N-28H	s2 100
s3	0.95	3245.3	STRE	7C-12H	s6 99
s4	9.44	3208.79	STRE	5C-10H	s4 96
s5	4.22	3187.24	STRE	3C-9H	s3 99
s6	14.46	3168.29	STRE	6C-11H	s5 95
s7	30.24	3124.1	STRE	14C-16H	s8 93
s8	12.9	3119.98	STRE	23C-24H	s14 11 s16 -79
s9	18.52	3112.63	STRE	23C-24H	s14 82 s16 11
s10	3.81	3111.76	STRE	23C-24H	s15 89
s11	51	3044.69	STRE	14C-15H	s7 -100
s12	11.01	3041.76	STRE	30C-31H	s12 93
s13	55.4	3035.62	STRE	20C-21H	s11 82
s14	8.96	3021.39	STRE	20C-22H	s10 90
s15	23.54	3002.66	STRE	20C-21H	s13 95
s16	74.16	2991.26	STRE	14C-17H	s9 93
s17	256.7	1763.07	STRE	26O-29C	256.70 1763.07 s17 81
s18	28.74	1673.2	STRE	1C-6C	s19 -50 s56 12
s19	56.74	1619.77	STRE	2C-3C	s23 -49 s58 -11
s20	10	1591.21	STRE	7C-8C	s18 -57
s21	261.79	1548.97	STRE	27N-29C	s24 -20 s36 51
s22	32.55	1517.76	BEND	15H-14C-17H	s23 -10 s41 -14
s23	100.32	1504.69	BEND	15H-14C-17H	s41 58 s70 17
s24	14.74	1498.59	BEND	21H-20C-22H	s45 -86
s25	6.77	1490.71	BEND	16H-14C-17H	s42 71 s71 18
s26	14.12	1490.48	BEND	16H-14C-17H	s49 -66 s77 22
s27	10.42	1489.47	STRE	6C-5C	s21 -15 s38 38
s28	1.77	1487.52	BEND	21H-20C-22H	s47 82
s29	48.49	1471.62	BEND	31H-30C-33H	s43 68
s30	7.39	1470.84	BEND	31H-30C-33H	s48 -75 s78 -10 s79 13
s31	4.1	1454.28	STRE	18N-1C	s25 13 s35 34
s32	4.65	1413.87	TORS	22H-20C-8C-7C	s73 55
s33	32.88	1398.32	BEND	31H-30C-32H	s50 86
s34	21.21	1379.48	STRE	1C-6C	s20 -24 s35 10 s75 -11
s35	31.4	1346.93	TORS	25H-23C-27N-29C	s20 -19 s75 11
s36	46.05	1332.96	BEND	24H-23C-27N	s44 55 s73 -10
s37	16.54	1326.2	STRE	18N-7C	s25 10 s26 20 s40 15
s38	62.63	1304.58	STRE	13O-4C	s27 15 s37 12 s38 -14 s75 12
s39	184.84	1266.88	STRE	27N-29C	s24 -21 s36 -12 s75 -10

s40	4.12	1262.22	BEND	12H-7C-8C	s38 11 s40 -16
s41	43.9	1237.11	BEND	9H-3C-4C	s26 -16 s75 -15
s42	50.86	1235.71	BEND	9H-3C-4C	s36 10 s37 -11 s46 30
s43	112.6	1228.99	BEND	9H-3C-4C	s27 -10 s37 10 s46 19 s70 -10
s44	44.25	1199.81	BEND	15H-14C-17H	s41 15 s70 48
s45	0.75	1170.8	BEND	16H-14C-17H	s42 24 s71 37 s72 -39
s46	0.65	1160.44	BEND	11H-6C-5C	s21 18 s39 56
s47	29.81	1116.22	STRE	18N-7C	s26 -26 s33 16 s40 25
s48	15.33	1110.4	STRE	27N-23C	s30 41
s49	46.42	1095.11	STRE	27N-23C	s30 14
s50	57.04	1079.41	STRE	13O-14C	s29 26
s51	14.54	1058.3	STRE	13O-14C	s29 -21 s32 -17 s37 14 s79 -11
s52	5.42	1051.94	TORS	33H-30C-29C-27N	s48 16 s79 -41 s90 17
s53	4.37	1024.44	STRE	23C-20C	s32 36
s54	8.02	991.12	TORS	31H-30C-29C-27N	s31 -19 s49 12 s77 -41
s55	7.75	934.75	BEND	7C-18N-1C	s22 -16 s57 20
s56	0.28	914.76	TORS	11H-6C-5C-4C	s68 75
s57	3.22	910.9	BEND	23C-27N-29C	s24 24 s31 15 s62 -14
s58	21.76	863.57	TORS	9H-3C-4C-5C	s66 74
s59	4.96	832.66	BEND	1C-6C-5C	s25 15 s28 18 s34 16
s60	5.02	810.92	TORS	12H-7C-8C-20C	s69 -72
s61	39.25	796.64	TORS	10H-5C-6C-1C	s67 61
s62	6.88	775.11	TORS	25H-23C-27N-29C	s69 -10 s76 36
s63	2.63	769.31	BEND	7C-18N-1C	s22 21 s57 22
s64	2.74	750.42	TORS	2C-3C-4C-5C	s81 -12 s83 -35
s65	10.92	723.31	STRE	8C-20C	s27 13 s28 16 s34 -10
s66	6.29	651.18	TORS	1C-6C-5C-4C	s81 -18
s67	3.4	642.06	TORS	1C-6C-5C-4C	s81 21 s90 -17
s68	3.08	631.05	OUT	26O-30C-27N-29C	s78 -13 s90 48
s69	2.64	614.67	BEND	26O-29C-30C	s31 21 s51 20 s62 10
s70	6.17	599.62	TORS	2C-1C-18N-7C	s85 47
s71	5.77	570.42	BEND	2C-3C-4C	s56 -12 s58 52
s72	17.26	474.84	BEND	6C-1C-18N	s59 39
s73	30.47	460.96	BEND	26O-29C-30C	s51 -22 s61 -11 s62 16 s65 25
s74	69.26	444.7	TORS	28H-27N-29C-30C	s65 -69
s75	2.11	436.43	TORS	1C-6C-5C-4C	s68 -10 s80 -62
s76	3.44	406.58	BEND	3C-4C-5C	s52 28 s53 14
s77	40.55	385.14	TORS	19H-18N-1C-2C	s64 46 s74 -10
s78	12.38	344.27	TORS	19H-18N-1C-2C	s91 -15 s93 51
s79	6.23	334.06	BEND	27N-23C-20C	s61 24 s93 11
s80	4.95	296.84	BEND	23C-27N-29C	s55 69
s81	31.13	268.83	TORS	19H-18N-1C-2C	s64 11 s92 38

s82	1.55	245.19	TORS	17H-14C-13O-4C	s71 -19 s72 -30 s91 13
s83	1.71	238.19	BEND	4C-13O-14C	s60 60
s84	5.29	199.59	BEND	23C-20C-8C	s63 24 s92 18
s85	2.44	167.33	TORS	2C-3C-4C-5C	s74 12 s91 28
s86	0.57	143.44	TORS	3C-4C-5C-6C	s81 13 s82 -45
s87	1.34	118.59	BEND	2C-3C-4C	s54 -25 s87 -19
s88	0.43	66.59	TORS	14C-13O-4C-3C	s78 38 s79 14 s86 -19
s89	4.64	64.82	TORS	14C-13O-4C-3C	s86 62
s90	10.44	54.34	TORS	7C-8C-20C-23C	s54 -12 s61 -11 s63 13 s87 22
s91	3.5	43.96	TORS	8C-20C23C-27N	s84 66 s88 -11
s92	0.6	36.09	TORS	7C-8C-20C-23C	s87 -13 s88 -48
s93	4.55	14.83	TORS	7C-8C-20C-23C	s89 72

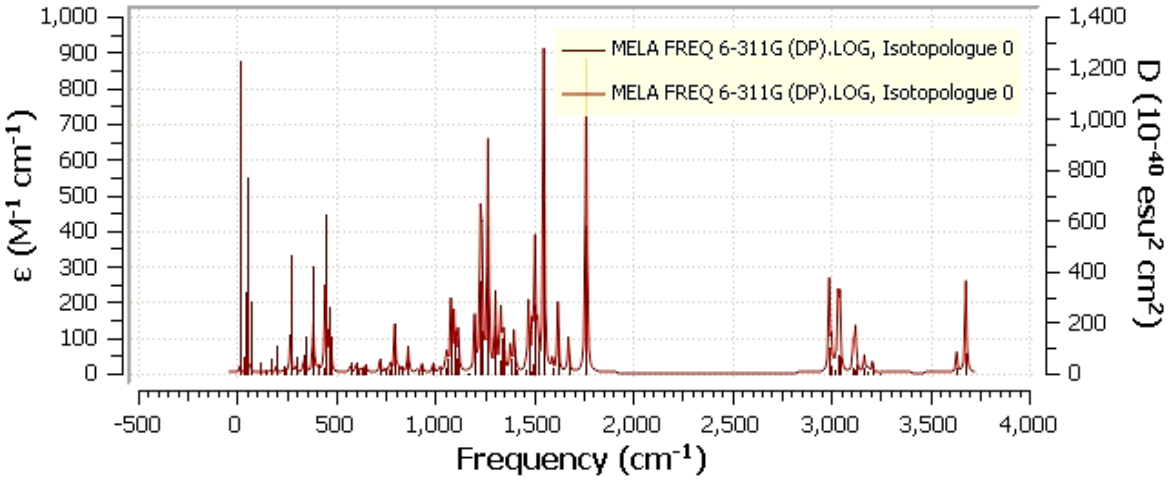

Fig. 3: IR spectrum of melatonin computed with DFT(B3LYP) at 6-311G(d,p) level.

experimental results quite well. Stretching vibrations in 23C-20C and 8C-20C, which are out of the ring, occurred at 1024.44 cm^{-1} and 723.31 cm^{-1}, respectively? Torsion in the C-C bond was observed at very low frequencies. The C–H stretching vibrations occur around 3000 and 3100 cm^{-1}.

Florio *et al.* (2002) reported in their study that the methoxy methyl group has three C-H stretching from 2800-3000 cm^{-1} region. In our calculation the stretching frequencies for methoxy group are 2991.26 cm^{-1}, 3044.69 cm^{-1}, 3124.1 cm^{-1} for 14C-17H, 14C-15H, 14C-16H, respectively. According to Trivedi *et al.* (2015) asymmetric C-H stretching vibrational peaks of indole were at 3022 cm^{-1} and 3049 cm^{-1}. In our DFT calculation C-H stretching for indole ring are 3168.29, 3187.24, 3208.79, 3245.3 for 6C-11H, 3C-9H, and 5C-10H, 7C-12H, respectively. The aromatic C=C strong stretching occurred at 1591.21 cm^{-1}. Vibrational peaks at 1673.2, 1619.77, 1591.21 are due to stretching of 1C-6C, 2C-3C, 7C-8C, respectively. The FT-IR region below 1000 cm^{-1} shows the out-of-plane bending of C-H bond vibrations in aromatic carbon double bonds (Tammer and Socrates, 2004). The carbonyl group shows a strong absorption band due to 26O-29C stretching vibration at 1763.07 cm^{-1}. Determining the C–N stretching mode of vibration is challenging since band mixing may occur in this area. C–N stretching vibration is typically detected in the range of 1300–800 cm^{-1} (Thamarai *et al*., 2020). However, the frequencies we observed are genuine and fall within the specified regions which are very close

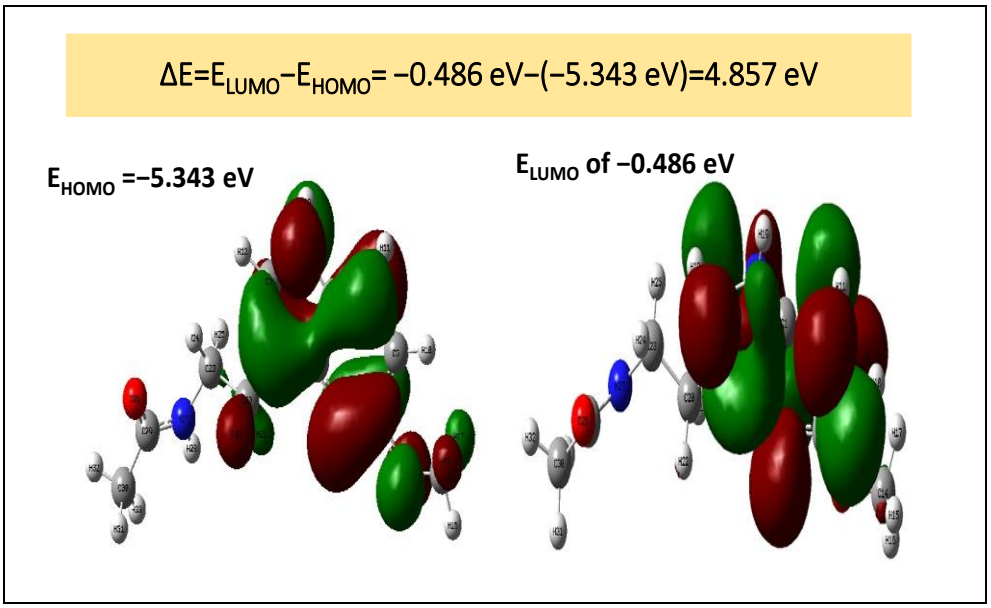

Fig. 4: HOMO and LUMO of Melatonin with DFT 6-311 G(d,p).

to the experimental data.

HOMO and LUMO

The highest occupied molecular orbitals (HOMO) and lowest unoccupied molecular orbital (LUMO) diagrams are shown in Figure 4. The molecular chemical stability is revealed by the energy difference between HOMO and LUMO. The negative charge is shown by the red colour whereas green represents the positive charge. The terms HOMO and LUMO refer to the donation and receiving of electrons, respectively. In this study, the orbital energy of HOMO and LUMO as well as the energy difference between LUMO and HOMO are measured using the B3LYP/6- 311G (d, p). Figure 4 shows 3D maps of the HOMO and LUMO orbitals for the melatonin compound. It shows how the orbitals for both HOMO and LUMO are located in the indole portion of melatonin. HOMO-LUMO energy gap describes the charge transfer within the molecule. For the title molecule, the colour green denotes a positive charge and the colour red a negative charge. The energy value for HOMO was −5.343 eV and for LUMO itwais −0.486 eV.

$\Delta E = E_{LUMO} - E_{HOMO}$, ΔE= −0.486 eV−(−5.343 eV)= 5.343−0.486=4.857 eV

Melatonin, with a E_{HOMO} −5.343 eV and E_{LUMO} −0.486 eV was fairly stable, having an energy gap of 4.857 eV. This stability is in agreement with its biological functions such as being an antioxidant, and explains moderate chemical activity. The electron density within the HOMO allow it to nuetralise free radicals, which is the requirement of its roles in oxidative stress protection.

Mulliken Atomic Charge Analysis

Figure 5 displays the net atomic charges at different atomic sites expressed in units of "e." These were found by using density functional theory (DFT) at the B3LYP level with a basis set of 6-311G (d, p) to Mulliken Population Analysis. The positive and negative values of the net charges at various atomic sites in a molecule reflect whether the total charges on the orbitals prior to the molecule's creation are larger or less than the free atomic charges. Highest negative charge was found on 13O (-0.359431), 18N (-0.448485), 26 O (-0.381197), N 27 (-0.414652) and 30 C (-0.302556). This means that the electron donating capacity is in the order 18N>N27>26O>13O and are the sites for electrophilic attack. On the other hand 29 C (0.317322) has highest positive charge on it and it is the most liable site for nucleophilic attacks.

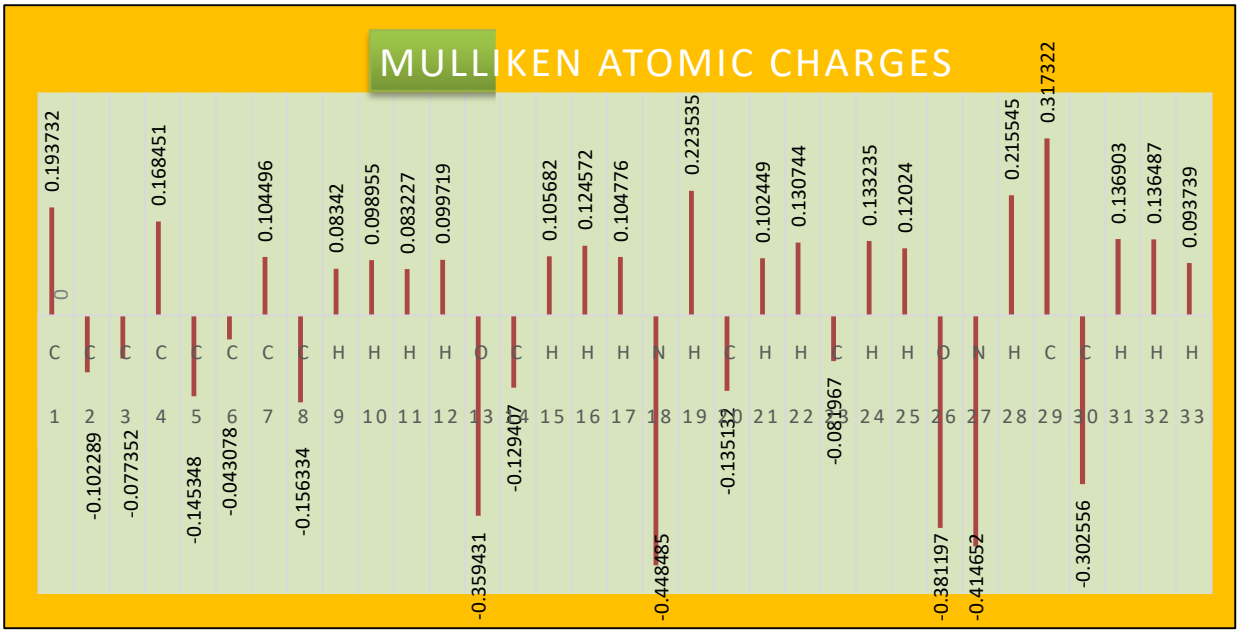

Fig. 5: Mulliken Atomic charges (e) of MTN calculated with DFT(B3LYP)/ 6-311 G(d,p).

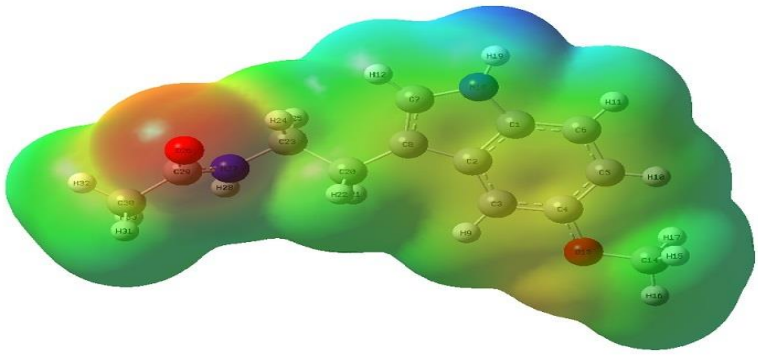

Fig. 6: MEP Surface of melatonin calculated with DFT 6-311 G(d,p).

MEP Surface Analysis

The net electrostatic effect generated at that location by the entire charge distribution surrounding the molecule is shown by the molecular electrostatic potential, or MEP (Vazquez-Vuelvas *et al*., 2011). Additionally, MEP surface is also helpful in identifying wide range of reactivity of a chemical compound such as inter-actions with hydrogen, electrophile, nucleo-phile and the investigation of biological reactivity (Muthu and Porchelvi, 2013; Sharma *et al*., 2019). It also aids in the visual comprehension of the molecule's relative polarity. By mapping electron density isosurface, it is used to find the size, shape, charge density, and reactive sites of the molecules. Different colours correspond to different levels of the electrostatic potential at the surface: red denotes the regions having maximum electro-negative potential, the highest positive potential is denoted by blue regions, and green denotes regions of zero potential. Red < orange < yellow < green < blue is the order in which electrostatic potential increases (Lakshminarayanan *et al*., 2021). As it is clear from MEP map that the intesity of red colour was more as compared to blue colour leads to the conclusion that there are more chances of an electrophilic attack (Fig. 6). The compound's colour code falls between $-4.618e^{-3}$ (red) and $+4.618e^{-3}$ (blue). The reactivity of melatonin is mainly due to indole and

Table 4: Electronic and Thermodynamic Properties of Melatonin Calculated with DFT/B3LYP at 6-311G (d, p) level

Parameters	Values
Electronic energy	-765.179579 Hartree
Electronic energy + Zero point energy	-764.907038 Hartree
Electronic energy + Thermal Energy correction	-764890128 Hartree
Electronic energy + Thermal Enthalpy correction	-764.889184 Hartree
Electronic energy + Thermal Free Energy correction	-764.954484 Hartree
E(Thermal)	181.633 kcal/mol
Heat Capacity	62.584 cal/mol-kelvin
Entropy	137.436 cal/mol-kelvin
Dipole Moment	3.237735 Debye
Polarizability (α)	167.741667 a.u.
Ionization Potential (IP)	IP=−HOMO=−(−5.343)= 5.343 eV
Electron Affinity (EA)	EA=−LUMO=−(−0.486)= 0.486 eV
Electronegativity (χ)	χ=IP+EA/2=2.9145 eV
Chemical Potential (μ)	μ=−χ =−2.9145 eV
Chemical Hardness (η)	η=IP−EA/2=2.4285 eV
Chemical Softness (S)	$S=1/\eta=0.4118\ eV^{-1}$
Electrophilicity Index (ω)	$\omega=\mu^2/2\eta=1.748$ eV

the acetyl ethylamine side chain. 18N-19H, indole is more prone to nucleophilic attack and the acetyl ethylamine side chain is more prone to elctrophilic attack in melatonin compound.

Electronic and Thermodynamic Parameters

Table 4 indicates the thermodynamic stability, electronic characteristics, and potential reactivity of melatonin. Melatonin is in a stable electronic structure, as evidenced by the low value of the electronic energy (−765.179579 Hartree), which indicates the ground state energy of the hormone. When quantum vibrational effect was taken into consideration, the corrected energy increased marginally to −764.907038 Hartree. This suggests that melatonin contributes to general stability by having a vibrational ground state that is near to its electrical ground state. Further evidence that melatonin stays stable under normal circumstances comes from the thermal energy correction −764.890128 Hartree and thermal free energy correction −764.954484 Hartree, which both display slight energy changes brought on by thermal influences. Melatonin's thermal energy of 181.633 kcal/mol indicates that it can maintain energy under normal temperature conditions without undergoing major structural changes. It can absorb a considerable amount of heat before altering owing to temperature, according to its heat capacity of 62.584 cal/mol-kelvin. From the entropy of Melatonin which is 137.436 cal /mol-kelvin, we can say that it has moderate degree of disorder at room temperature. This relatively low value of the dipole moment, 3.24 Debye, suggests that at least this molecule is partially polar which would explain its relative stability in biological milieus and in polar solvents. Furthermore its Polarizability (167.74 a.u.) indicates that it can be polarized under an electric field which shows that it is stable when interacting with other molecules or solvents. From these values, we can say that melatonin is a stable molecule both electronically and thermodynamically which makes it suitable for biological and pharmaceutical applications.

Table 5: Molecular docking results showing binding sites and binding score when melatonin is docked with different cancer protein targets

S. No.	Target	PDB-ID	Binding sites			Binding energy kcal/mol
			x	y	z	
1	MMP13 Collagenase 3	1xuc	-11.3806	26.3613	47.273	-8.2
2	Matrix metalloproteinase-9	2ow2	69.2737	17.371	54.3287	-8.1
3	EGFR	1xkk	17.7346	33.8996	37.9079	-7.3
4	NUDT5_HUMAN(ADP-sugar pyrophosphatase)	2dsd	1.7047	14.1815	69.2225	-7.7

Melatonin's reluctance to lose electrons is shown by a higher IP and electronegativity, whereas its capacity to receive electrons in reactions is suggested by the electrophilicity index. Melatonin's moderate chemical hardness and softness indicate balanced reactivity because it is neither too hard nor too soft.

Docking Studies

Melatonin has recently emerged as one of the most promising drugs due to its functions in tumour biology and treatment. Some of the benefits of this hormone include alteration of main signaling pathways, protection during chemotherapy, and improvement in overall quality of life in patients. These pathways include PI3K, NF-κB, and Wnt/β-Catenin. This ability to change such pathways begs the possibility that melatonin may interfere with a number of cellular functions, including immune response, metastasis-that is, the spreading of cancer-and apoptosis, or programmed cell death-an important aspect of cancer biology (Yi *et al.*, 2024). Melatonin has demonstrated encouraging results in lowering oxidative stress, inflammation, and hormonal imbalances in gynaecological disorders as endometriosis, polycystic ovarian syndrome (PCOS), and uterine leiomyoma (Hosseinzadeh *et al.*, 2024). In this study the melatonin was docked with different targets like Matrix metalloproteinase-9, EGFR, MMP13 Collagenase 3 and NUDT5_HUMAN (ADP-sugar pyrophosphatase). We have observed binding score <-7 for all the protein targets as shown in Table 5. The least binding score is shown by MMP13 Collagenase 3 which means it has highest binding affinity.

MMP13 plays a role in the breakdown of extracellular matrix and is linked to the invasion and spread of cancer. As shown in Table 5, on docking melatonin with MMP 13, we got binding Score of -8.2, which proves that melatonin has very high affinity to bind with MMP 13 (Fig. 7). Melatonin and MMP13 have a strong binding score (-8.2), which implies that melatonin may suppress MMP13's function, lowering the risk of tumour invasion and metastasis. This might help in stopping the spread of cancer cells, especially in malignancies like breast and prostate cancers that mainly depend on matrix breakdown. Furthermore docking of melatonin with Matrix Metalloproteinase-9 (MMP-9) has shown binding Score of -8.1. This means melatonin has high binding affinity with MMP-9 (Fig. 7). MMP9 is essential for the breakdown of the extracellular matrix, which is necessary for the invasion and metastasis of cancer cells. Melatonin may reduce the enzymatic activity of MMP-9, which could lessen the metastatic spread of cancer cells. This inhibition may lessen the chance of metastasis and delay the growth of the tumor. In a number of cancers EGFR is over-expressed and it plays very important role in the proliferation, survival, and angiogenesis of tumor cells. So, we have docked melatonin with Epidermal Growth Factor Receptor (EGFR) and found the binding score of -7.3 (Fig. 8). It again

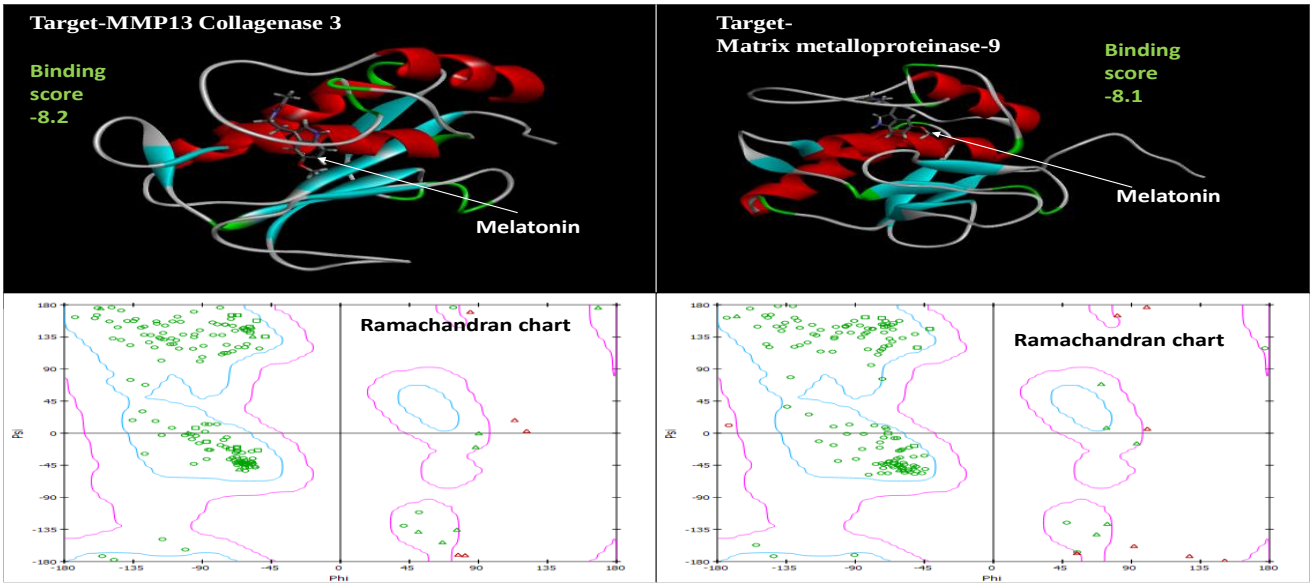

Fig. 7: Binding of melatonin with MMP13 Collagenase 3 and Matrix metalloproteinase-9 with their respective binding scores and Ramachandran plots.

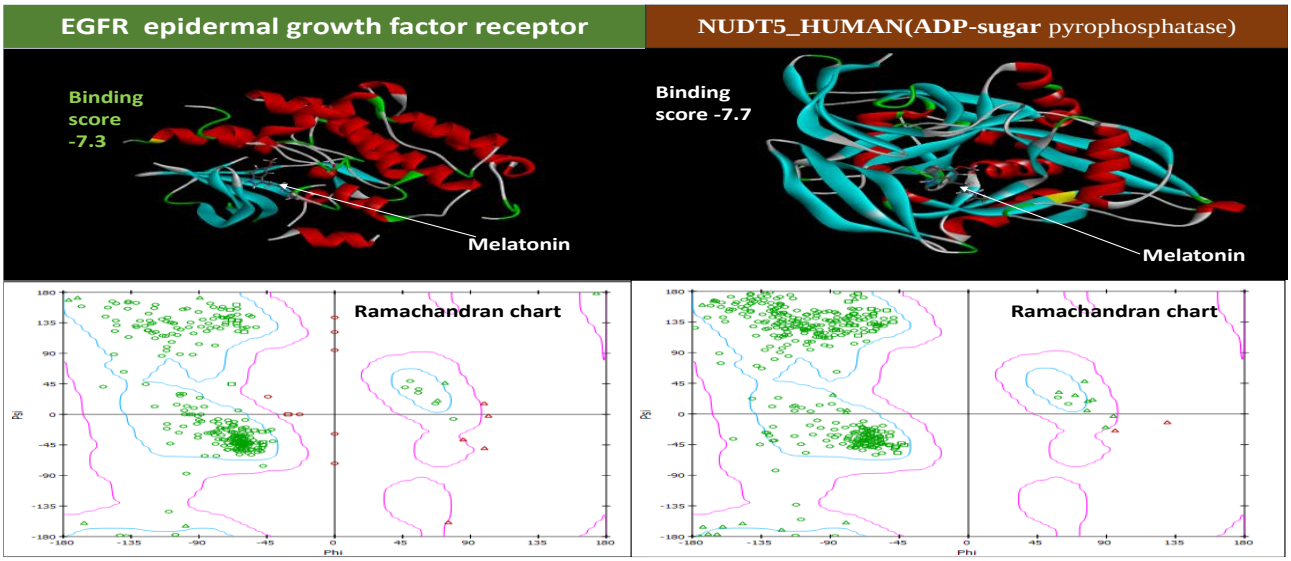

Fig. 8: Binding of melatonin with EGFR andNUDT5_HUMAN (ADP-sugar yrophosphatase) with their respective binding scores and Ramachandran plots.

revealed that melatonin has high binding affinity with EGFR. This means that melatonin has high potential to be an EGFR antagonist and, therefore, may inhibit the proliferation of malignant cells and the development of tumors. Hence, melatonin has good therapeutic properties for cancer treatment in patients with lung and breast cancers where cancer is driven by EGFR.

Cancer cell survival depends on energy homeostasis and metabolism, both of which are mediated by NUDT5. Melatonin may interfere with the metabolic pathways that support the growth and spread of cancer by targeting NUDT5. A potentially strong interaction is indicated by the binding score of -7.7, which implies that melatonin may hinder the energy production of cancer cells, resulting in either decreased growth or death (Fig. 8). As it is clear from the Ramachandran plots showed that most of the residues remain in the preferred and allowed regions, the binding of

melatonin to Matrix metalloproteinase-9,MMP13 Collagenase 3, EGFR and NUDT5_HUMAN(ADP-sugar pyrophosphatase) appears to maintain the protein's structural stability (Figs., 7, 8). This implies that in this interaction the receptor is not under a lot of pressure.

MTN shows interactions with major signaling pathways, including PI3K, NF-κB, and Wnt/β-Catenin. The growth and spread of tumours depend on these pathways, and MTN has tendency to alter them. This means it may have an impact on vital cellular processes such as immunological responses, metastasis, and apoptosis (Yi *et al.*, 2024). Melatonin therapy has led to a decrease in the patient's PSA levels, which may be considered as an oncostatic effect. Melatonin can reduce symptoms of polyneuropathy and normalize inflammation markers, two of the main side effects of chemotherapy (Smorodin *et al*., 2024). Melatonin is capable of showing anti-tumor activity after administration with CML cell lines, most highly expressed in K562 cell lines representing a model for CML. Melatonin was significantly inhibitory at concentrations above 0.1 μM, reducing the cell growth by a mean value of 74.7% inhibition at 1 μM. It is likely to be a useful fertoprotective drug to preserve gonadal function without diminishing the anticancer properties of medications like imatinib when a strategy is needed to reduce the gonadotoxicity caused by chemotherapy (Addison *et al*., 2024). Hub genes involved in several cancer pathways that were identified by the study include STAT3, JUN, TP53, among others. It found higher associations of the changes of the melatonin-related signaling pathway with many different cancers, such as breast and hepatic cancer and prostate and oral cancer. Melatonin, therefore, may potentially target various other cancerous diseases (Chuffa *et al*., 2023).

Conclusion

Melatonin has wide anticancer activity that includes the modulation of immune response, regulation of cell cycle and apoptosis, antioxidant effects, as well as inhibition of angiogenesis. It can bind to major proteins of cancerous invasion, metastasis, and development, based on the docking results. Melatonin exhibits promising binding affinities towards many critical proteins involved in the processes of cancer. While its interactions with EGFR receptors are promising within the modulation of tumour growth and proliferation, its significant interactions with MMP-9 and MMP13 suggest a role in the inhibition of metastasis. Finally, the inhibition of NUDT5 could indicate that melatonin interferes somehow with metabolism in cancer cells. All these aspects together, however, allow this complex approach of melatonin to be a helpful adjuvant in the therapy of cancer.

Although promising, much more research should be done to fully understand the mechanisms involved and to optimize the therapeutic applications of melatonin in oncology. More extensive and systematic research needs to be conducted in order to establish greater knowledge on the systemic effects of melatonin as far as cancer treatment is concerned. This will include any association to survival rates as well as its capability to reduce side effects caused by drugs. This study may become an important constituent of future cancer treatment by integrating the work done till history with ongoing studies. It calls for more investigation in the role of melatonin within cancer treatment and suggests a greater role in treating strategies in the near future. The remarkable positivity obtained from these results *in vitro* have stressed on further research by the study itself. The complexity in drug interaction, such as metabolic and distribution aspects, poses a challenge in a clinical setting; hence, these studies need to be done using an animal model before the actual drug administration in human clinical trials. In summary, melatonin presents a lot of promise as a supportive treatment for cancer patients; however, more study is expected in efforts to gain full understanding about its efficacy and optimally utilized for the right clinical settings.

Acknowledgements

Authors express great gratitude to the Hon'ble Chancellor of Guru Kashi University for his support in facilitating this collaborative research.

Conflict of Interest

The authors declare no conflicts of interest.

References

Addison WA, Alley C, Bold JG and Letourneau JE. (2024) P-373 Melatonin and chemotherapy: Does the proposed fertoprotective agent impair the anti-tumor effects of cancer therapy? Hum Reprod. 39(Supplement_1): deae108.729.

Altun A, Gölcük K and Kumru M. (2003) Structure and vibrational spectra of p-methylaniline: Hartree-Fock, MP2 and density functional theory studies.Journal of Molecular Structure: THEOCHEM.637(1–3):155-169,

Arendt J. (1998) Melatonin and the pineal gland: influence on mammalian seasonal and circadian physiology. Rev Reprod. 3: 13-22.

Bartsch C, Bartsch H, Jain AK, Laumas KR and Wetterberg L. (1981) Urinary melatonin levels in human breast cancer patients. J Neural Transm. 52: 281-294.

Bisong EA, Louis H, Unimuke TO, Odey JO, Ubana EI, Edim MM, Tizhe FT, Agwupuye JA and Utsu PM (2020). Vibrational, electronic, spectroscopic properties, and NBO analysis of p-xylene, 3,6-difluoro-p-xylene, 3,6-dichloro-p-xylene and 3,6-dibromo-pxylene: DFT study. Heliyon 6(12): e05783.

Bonomini F, Borsani E, Favero G, Rodella L and Rezzani R. (2018) Dietary melatonin supplementation could be a promising preventive/therapeutic approach for a variety of liver diseases. Nutrients 10(9): 1135.

Brown DG and Bostrom J. (2016) Analysis of past and present synthetic methodologies on medicinal chemistry: where have all the new reactions gone? J Med Chem. 59: 4443-4458.

Brunton L, Chabner B and Knollman B. (2010) Goodman and Gilman's the pharmacological basis of therapeutics. McGraw-Hill, New York, NY.

Cecon E, Oishi A and Jockers R. (2018) Melatonin receptors: molecular pharmacology and signaling in the context of system bias. Br J Pharmacol. 175: 3263-3280.

Checkley SA, Murphy DGM, Abbas M, Marks M, Winton F, Palazidou E, Murphy DM, Frany C, Binmey C and Costa DC. (1993) Melatonin rhythms in seasonal affective disorder. Br J Psychiatry 163: 332-337.

Chuffa L, Carvalho R, Camargo VL, Cury S, Domeniconi R, Zuccari DA and Seiva FR. (2023) Melatonin and cancer: Exploring gene networks and functional categories. Melatonin Research 6(4): 431-451.

Claustrat B, Brun J and Chazot G. (2005) The basic physiology and pathophysiology of melatonin. Sleep Med Rev. 9: 11-24.

Coleman MP and Reiter RJ. (1992) Breast cancer, blindness and melatonin. Eur J Cancer 28: 501-503.

Dubocovich ML, Delagrange P, Krause DN, Sugden D, Cardinali DP and Olcese J. (2010) International Union of Basic and Clinical Pharmacology. LXXV. Nomenclature, classification, and pharmacology of G protein-coupled melatonin receptors. Pharmacol Rev. 62: 343-380.

Florio GM, Christie RA, Jordan KD and Zwier TS. (2002) Conformational preferences of jet-cooled melatonin: Probing tran- and cis-amide regions of the potential energy surface. J Am Chem Soc. 124: 10236-10247.

Frisch MJ, Frisch M, Trucks G, Schlegel K, Scuseria G, Robb M, Cheeseman J, Montgomery J, Vreven T, Kudin KN, Burant J, Millam J, Iyengar S, Tomasi J, Barone V, Mennucci B, Cossi M, Scalmani G, Rega N, Petersson A, Nakatsuji H, Hada M, Ehara M, Toyota K, Fukuda R, Hasegawa J, Ishida M, Nakajima T, Honda Y, Kitao O, Nakai H, Klene M, Li X, Knox J, Hratchian H, Cross D, Bakken V, Adamo C, Jaramillo-Merchan J, Gomperts R, Stratmann R, Yazyev O, Austin A, Cammi R, Pomelli C, Ochterski J, Ayala P, Morokuma K, Voth G, Salvador P, Dannenberg JJ, Zakrzewski VG, Dapprich S, Daniels AD, Strain M, Farkas O, Malick S, Rabuck A, Raghavachari K, Foresman J, Ortiz J, Cui Q, Baboul AG, Clifford S, Cioslowski J, Stefanov B, Liu G, Liashenko A, Piskorz P, Komaromi I, Mata R, Fox D, Keith T, Laham S, Peng CY, Nanayakkara A, Challacombe M, Gill P, Johnson B, Chen W, Wong M, Rodríguez-Salinas González, Pople J, Dannenberg J, Zakrzewski V, Daniels A, Baboul AG, Peng Y, Scuseria GE, Millam JM, Foresman JB, Frisch MJ, Montgomery JA, Stratmann RE, Malick DK, Li XB, Todd K, Wong MW, Schlegel HB, Ayala PY, Stefanov BB, Hada M, Martin RL, Kudin KN, Hratchian HP, Voth GA, Austin AJ, Strain MC, Adamo C, Gill PMW, Robb MA, Petersson GA, Cross JB, La Torre J, Trucks GW, Burant JC, Fox DJ, Rabuck AD, Huerta C, Akhras M, Cheeseman JR, Iyengar SS, Pople JA, Knox JE, Ochterski JW and Johnson BA. (2005) Gaussian 03, Revision D. I. Gaussian Inc., Wallingford.

Greenberg A, Breneman CM and Liebman JF. (2000) The amide linkage: structural significance, chemistry, biochemistry, and material science. Wiley, New York, NY.

Hardeland R, Cardinali DP, Srinivasan V, Spence DW, Brown GM and Pandi-Perumal SR. (2011)

Melatonin-- A pleiotropic, orchestrating regulator molecule. Prog Neurobiol. 93: 350-384

Herxheimer A and Petrie KJ. (2002) Melatonin for the prevention and treatment of jet lag. Cochrane Database Syst Rev. https://doi.org/10.1002/14651858.CD001520

Hosseinzadeh A, Alinaghian N, Sheibani M, Seirafianpour F, Jamshidi Naeini A and Mehrzadi S. (2024) Melatonin: Current evidence on protective and therapeutic roles in gynecological diseases. Life Sci. 344: 122557.

Hughes AB. (2009) Amino acids, peptides, and proteins in organic chemistry. Wiley-VCH, Weinheim, Germany.

Imenshahidi M, Karimi G and Hosseinzadeh H. (2020) Effects of melatonin on cardiovascular risk factors and metabolic syndrome: a comprehensive review. Naunyn Schmiedebergs Arch Pharmacol. 393: 521-536.

Kaspar AA and Reichert JM. (2013) Drug future directions for peptide therapeutics development. Drug Discov Today 18: 807-817.

Kemnitz CR and Loewen MJ. (2007) Amide resonance correlates with a breadth of C-N rotation barriers. J Am Chem Soc. 129: 2521-2528.

Lakshminarayanan S, Jeyasingh V, Murugesan K, Selvapalam N and Dass G. (2021) Molecular electrostatic potential (MEP) surface analysis of chemo sensors: An extra supporting hand for strength, selectivity and non-traditional interactions. J Photochem Photobiol. 6: 100022.

Lerner AB, Case JD and Takahashi Y. (1958) Isolation of melatonin, the pineal gland factor that lightens skin color. J Am Chem Soc. 80: 2587-2588.

Mahesh S, Tang KC and Raj M. (2018) Amide bond activation of biological molecules. Molecules 23: 2615.

Mujika JI, Mercero JM and Lopez X. (2005) Water-promoted hydrolysis of a highly twisted amide: rate acceleration caused by the twist of the amide bond. J Am Chem Soc. 127: 4445-4453.

Muthu S and Porchelvi EE. (2013) FTIR, FT-RAMAN, NMR, spectra, normal co-ordinate analysis, NBO, NLO and DFT calculation of N,N-diethyl-4-methylpiperazine – 1 - carboxamide molecule. Spectrochim Acta A Mol Biomol Spectrosc. 115: 275-286.

Nishi T, Saeki K, Miyata K, Yoshikawa T, Ueda T, Kurumatani N, Obayashi K and Ogata N. (2020) Effects of cataract surgery on melatonin secretion in adults 60 years and older: a randomized clinical trial. J Am Med Asso Ophthalmol. 138: 405-411.

Pattabiraman VR and Bode JW. (2011) Rethinking amide bond synthesis. Nature 480: 471-479.

Rebollo-Hernanz M, Aguilera Y, Herrera T, Cayuelas T, Dueñas M, Rodríguez-Rodríguez P, Ramiro-Cortijo D, Arribas SM and Martín-Cabrejas MA. (2020) Bioavailability of melatonin from lentil sprouts and its role in the plasmatic antioxidant status in rats. Foods 9: 330.

Reiter RJ, Mayo JC, Tan DX, Sainz RM, Alatorre-Jimenez M and Qin L. (2016) Melatonin as an antioxidant: under promises but over delivers. J Pineal Res. 61: 253-278.

Sharma A, Singh OP, Sharma AK, Kumar A and Sharma AK. (2019) Ab-initio study of vibrational spectra revealed the better reactive potential of eugenol over carvacrol: bioactive compounds derived from *Ocimum tenuiflorum* (Tulsi). Int J Pharm Res. 11: 147-151

Smorodin E, Chuzmarov V and Veidebaum T. (2024) The potential of integrative cancer treatment using melatonin and the challenge of heterogeneity in population-based studies: A case report of colon cancer and a literature review. Curr Oncol. https://doi.org/.3390/curroncol31040149

Srinivasan V, Smits M, Spence W, Lowe AD, Kayumov L, Pandi-Perumal SR, Parry B and Cardinali DP. (2006) Melatonin in mood disorders. World J Biol Psychiatry 7: 138-151.

Talib W, Alsayed A, Abuawad A, Daoud S and Mahmod A. (2021) Melatonin in cancer treatment: current knowledge and future opportunities. Molecules 26: 2506.

Tammer M and Socrates G. (2004). Infrared and Raman characteristic group frequencies: Tables and Charts. Colloid Polym Sci. 283: 235.

Tan DX, Manchester LC, Terron MP, Flores LJ and Reiter RJ. (2007) One molecule, many derivatives: a never-ending interaction of melatonin with reactive oxygen and nitrogen species? J Pineal Res. 42: 28-42.

Tarı GÖ and Aydemir E. (2023) Experimental and DFT study of (E)- 4 - bromo- 2(((3-chloro – 4 - (4-chlorophenoxy) phenyl) imino) methyl)-5-fluorophenol: molecular and electronic properties in solvent media. J Mol Struct. 1277: 134880.

Thamarai A, Vadamalar R, Raja M, Muthu S, Narayana B, Ramesh P, Muhamed RR, Sevvanthi S and Aayisha S. (2020) Molecular structure interpretation, spectroscopic (FT-IR, FT-Raman), electronic solvation (UV-Vis, HOMO-LUMO and NLO) properties and biological evaluation of (2E)-3-(biphenyl-4-yl)-1-(4bromophenyl) prop-2-en-1-one: Experimental and computational modeling approach. Spectrochim Acta A Mol Biomol Spectrosc. 226: 117609.

Thorner J, Emr SD and Abelson JN. (2000) Applications of chimeric genes and hybrid proteins part A: gene expression and protein purification. Methods Enzymol. 326: 601-617.

Touitou Y, Arendt J and Pevet P. (1993) Melatonin and the pineal gland-- From basic science to clinical application. Elsevier, New York, NY.

Trivedi M, Tallapragada RM, Branton A, Trivedi D, Nayak G, Mishra R and Jana S. (2015) Biofield treatment: A potential strategy for modification of physical and thermal properties of indole. J Environ Anal Chem 2: 152.

Vazquez-Vuelvas OF, Hernandez-Madrigal JV, Gavino R, Tlenkopatchev MA, Morales-Morales D, Germán-Acacio JM, Gómez-Sandoval Z, Garcias-Morales C, Ariza-Castolo A and Pineda-Contreras A. (2011) X-ray, DFT, FTIR and NMR structural study of 2, 3-dihydro-2-(R-phenylacylidene)-1, 3, 3-trimethyl-1H-indole. J Mol Struct. 987: 106-118.

Vlachou M, Siamidi A, Dedeloudi A, Konstantinidou SK and Papanastasiou IP. (2021) Pineal hormone melatonin as an adjuvant treatment for COVID-19. Int J Mol Med. 47(4): 47.

Wang B and Cao Z. (2011) Acid-catalyzed reactions of twisted amides in water solution: competition between hydration and hydrolysis. Chem Eur J. 17: 11919-11929.

Yi YJ, Tang H, Pi PL, Zhang HW, Du SY, Ge WY, Dai Q, Zhao ZY, Li J and Sun Z. (2024) Melatonin in cancer biology: Pathways, derivatives, and the promise of targeted delivery. Drug Metab Rev. 56(1): 62-79.

Zhang JJ, Meng X, Li Y, Zhou Y, Xu DP, Li S and Li HB. (2017) Effects of melatonin on liver injuries and diseases. Int J Mol Sci. 18: 673.